

Higher-Order Effects in Electron-Nucleus Scattering*

CHRISTIAN TOEPFFER AND WALTER GREINER

*Department of Physics, University of Virginia, Charlottesville, Virginia and
Institut für Theoretische Physik der Universität Frankfurt, Frankfurt/Main, Germany*

(Received 4 November 1968)

Higher-order effects are calculated in the framework of the eigenchannel theory for elastic and inelastic electron-nucleus scattering in the energy region $100 \leq E \leq 250$ MeV. A dispersion effect of about 12% is found for the elastic scattering on Ni^{58} at a momentum transfer $q \approx 500$ MeV/c. For inelastic scattering, the reorientation effect is discussed, in addition to the dispersion effect. The total higher-order effect changes the form factor for a hindered first-order transition by 50% at its minima. Furthermore, the dependence of the higher-order effects on the transition potentials of the virtual excitations, the model dependence, and the dependence on the energy E of the electron and the momentum transfer q are discussed. A closed formula for the S matrix is developed by calculating the eigenchannels in stationary perturbation theory.

I. INTRODUCTION

HIGH-ENERGY electron-nucleus scattering has been proved to be a successful tool for investigations of the nuclear structure. The main reason for this is that the interaction between the electron and the nucleus is well known, which facilitates the analysis of the scattering data. Besides the earlier more general review articles of Hofstadter,¹ we refer in this connection to the review paper of De Forest and Walecka² on the theoretical aspects of electron-nucleus scattering.

The analysis of a scattering experiment is made in the following manner: One assumes a nuclear model with certain charge, current, and magnetization density distributions and calculates the cross section in first-order perturbation theory, where either the electron is treated as a free particle [Born approximation (BA)] or the static Coulomb field is taken into account exactly^{3,4} [distorted-wave Born approximation (DWBA)].

An open question was: How much are the results modified by taking into account higher-order effects in which two or more virtual quanta are exchanged between the electron and the nucleus? Estimates were made in second-order Born approximation.^{5,6} It has been pointed out, however,⁵ that one has to start with correct, i.e., distorted, wave functions to get reliable results on the higher-order effects.

This was done by Rawitscher,⁷ who considered a

virtual monopole excitation in a coupled-channel calculation for the elastic scattering of 250-MeV electrons by Ca^{40} . A relative effect of $\approx 5\%$ is found at those scattering angles where the elastic cross section has minima (Fig. 14). Recently, second-order perturbation theory with distorted waves was employed by Onley.⁸

Related to the coupled-channel method is the eigenchannel theory (EKT) of Danos and Greiner,⁹ and co-workers,⁹ which has been applied to a number of nuclear reactions.⁹ The EKT has also been formulated for high-energy electron-nucleus scattering,^{10,11} where, in contrast to the case of nuclear reactions, the S matrix can be found after a single iteration. First results, which have been reported elsewhere,¹² showed that higher-order effects give contributions up to 10–25% to elastic and 50–100% to inelastic form factors for a target nucleus with $Z=26$ and an incident electron energy of $E=200$ MeV.

In order to give here a more complete investigation of the higher-order effects, we present in Sec. II the EKT construction scheme for the S matrix. By applying stationary perturbation theory we are then able to derive in Sec. III a closed formula for the S matrix which illuminates some of our later results. In Sec. IV we specify the nuclear model. The following properties of higher-order effects in elastic scattering are then treated in Sec. V: the dependence of the effect on the properties of the intermediate transition potentials, the atomic weight A , and the nuclear model. Furthermore, the effect is calculated as a function of both the incident electron E and the momentum transfer q . In

* Work supported in part by the Deutsche Forschungsgemeinschaft with a contract for studies on nuclear structure and carried out under the auspices of the Center for Advanced Studies at the University of Virginia; also supported by a computer grant from the Computer Science Center of the University of Virginia.

¹ *Electron Scattering and Nuclear and Nucleon Structure*, edited by R. Hofstadter (W. A. Benjamin, Inc., New York, 1963); R. Hofstadter, *Rev. Mod. Phys.* **28**, 214 (1956).

² T. De Forest and J. D. Walecka, *Advan. Phys.* **15**, 1 (1966).

³ D. R. Yennie, D. G. Ravenhall, and R. N. Wilson, *Phys. Rev.* **95**, 500 (1954).

⁴ T. A. Griffy, D. S. Onley, J. T. Reynolds, and L. C. Biedenharn, *Phys. Rev.* **128**, 833 (1962).

⁵ L. I. Schiff, *Phys. Rev.* **98**, 756 (1955).

⁶ A. Bottino, G. Ciochetti, and A. Molinari, *Nucl. Phys.* **89**, 192 (1966).

⁷ G. H. Rawitscher, *Phys. Rev.* **151**, 846 (1966).

⁸ D. S. Onley, *Nucl. Phys.* **A118**, 436 (1968).

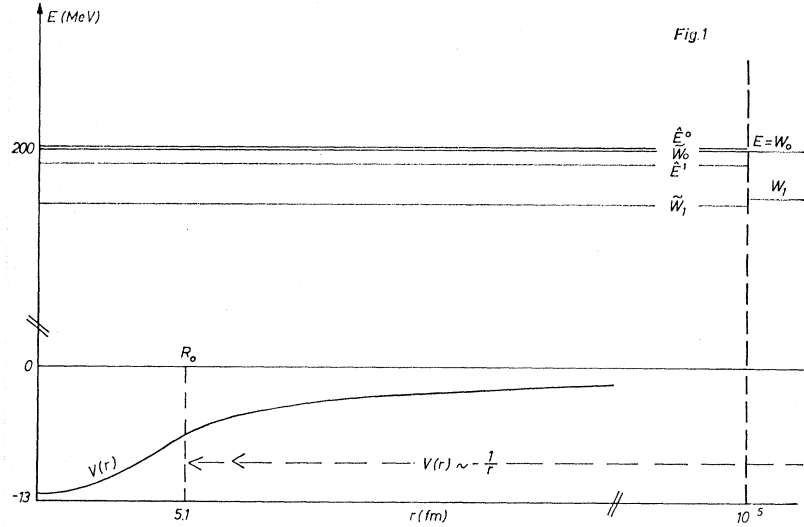
⁹ M. Danos and W. Greiner, *Phys. Rev.* **146**, 708 (1966); P. P. Delsanto, H. G. Wahsweiler, and W. Greiner, *Phys. Rev. Letters* **19**, 706 (1967); A. Piazza, H. G. Wahsweiler, and W. Greiner, *Phys. Letters* **25B**, 579 (1967); C. Mahaux and H. A. Weidenmüller, *Phys. Rev.* **170**, 847 (1968); H. G. Wahsweiler, W. Greiner, and M. Danos, *ibid.* **170**, 893 (1968); P. P. Delsanto, M. F. Roetter, and H. G. Wahsweiler, *Z. Physik* **222**, 67 (1969).

¹⁰ C. Toepffer, thesis, Frankfurt/Main, 1967 (unpublished).

¹¹ C. Toepffer and W. Greiner, *Ann. Phys. (N.Y.)* **47**, 285 (1968).

¹² C. Toepffer, *Phys. Letters* **26B**, 426 (1968).

FIG. 1. Inner and outer space for the construction of the S matrix. Because of the matching condition at $a=10^5$ fm, the inner energy \tilde{W}_1 of the electron does not coincide with $W_1=E-E_{N,1}$. Because of the coupling of the channels, the energies \hat{E}^0 and \hat{E}^1 do not coincide with E . This can be reached by a renormalization of the eigenphases.



Sec. VI, the corresponding investigations are made for inelastic scattering. Up to this point we have considered only virtual transitions to nuclear states other than the initial and the final—a situation in which the higher-order effect is called (in analogy to optics) a dispersion effect. However, under certain circumstances it is also possible that virtual transitions occur between the various magnetic substates of a nuclear state. This effect is well known from Coulomb excitation and is called the reorientation effect. This effect is discussed in Sec. VII together with the dispersion effect. Details on the numerical accuracy of our program are given, along with a comparison of our results with those of other authors, in Sec. VIII. In Sec. IX the results are summed up and some conclusions are drawn.

II. EIGENCHANNEL THEORY FOR ELECTRON SCATTERING

For the construction of the S matrix, we divide the total Hamiltonian H of the scattering problem into

$$\begin{aligned} H &= H_{\text{target}} + H_{\text{particle}} + H_{\text{int}} \\ &= H_0 + H_{\text{int}} \end{aligned} \quad (1)$$

and look for eigenfunctions ψ of H that become superpositions of eigenfunctions of H_0 in the asymptotic region, where H_{int} is supposed to be negligible:

$$\psi \sim \sum_c (A_c I_c + B_c O_c) \varphi_c. \quad (2)$$

Here I_c and O_c are the ingoing and outgoing spherical waves of the particle, and φ_c is a channel wave function, i.e., the wave function of the nucleus coupled with the spin-angular part of the wave function of the electron.

The S matrix transforms the amplitudes of the

incoming into the amplitudes of the outgoing waves:

$$B_c = - \sum_{c'} S_{cc'} A_{c'}. \quad (3)$$

Thus (2) becomes

$$\psi \sim \sum_c (A_c I_c - \sum_{c'} S_{cc'} A_{c'} O_{c'}) \varphi_c. \quad (4)$$

The amplitudes A_c are determined by the condition that ψ should describe a plane wave in the entrance channel.

Time-reversal invariance implies that the S matrix is unitary. Moreover, its submatrices $S^{I,\pi}$ of a given total spin I and parity π are symmetric.¹³ Therefore, $S^{I,\pi}$ can be diagonalized by the real, orthogonal matrix $V_c^{I,\pi,\nu}$, and the following eigenvalue equation exists:

$$\sum_{c'} S_{cc'}^{I,\pi} V_c^{I,\pi,\nu} = \exp(2i\delta^{I,\pi,\nu}) V_c^{I,\pi,\nu}. \quad (5)$$

The phases $\delta^{I,\pi,\nu}$ are the eigenphases, and ν denotes the various eigenchannels, of which there are as many as there are open physical channels. Assuming that the amplitudes A_c of the incoming channels are the $V_c^{I,\pi,\nu}$,¹⁴ the wave function in the ν th eigenchannel is

$$\psi \sim \sum_c V_c^\nu (e^{-i\delta^\nu} I_c - e^{i\delta^\nu} O_c) \varphi_c. \quad (6)$$

For the further evaluation of this expression, we have to specify the physical channels $\{c\}$.

We assume that the target nucleus has a set of discrete energy levels $\{\alpha, J^\pm\}$, which are labeled by the index α , so that the nuclear spin J is a redundant index. Since we deal with relativistic electrons as probing

¹³ E. P. Wigner, *Group Theory* (Academic Press Inc., New York, 1959).

¹⁴ Because we will subsequently always consider the subspaces of fixed total spin I and parity π , we will drop the indices I and π whenever no ambiguity arises.

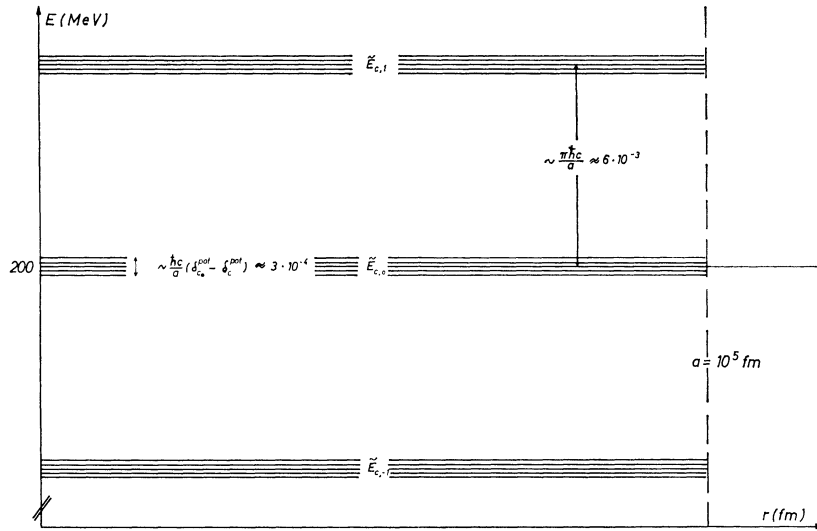


FIG. 2. Enlarged section of Fig. 1, showing how the unperturbed total inner energies $E_{c,n}$ are arranged in multiplets. Since the perturbation is small, the perturbed energies $\tilde{E}_{c,n}$ are arranged in similar multiplets. The differences $\tilde{E}_{c,0} - E_{c,0}$ are of the order 3×10^{-4} MeV and are thus much smaller than the energy loss of the electrons in the excitation of an intermediate state.

particles, the Hamiltonian H_0 is given by

$$H_0 = H_{\text{nucleus}} + H_{\text{Dirac}}, \quad (7)$$

and the electrostatic field of the nucleus has to be included in H_{Dirac} because of its long-range properties. Making a partial-wave decomposition of the wave functions, we have in the asymptotic region, where $k_\alpha r \gg l(l+1)$, and in the high-relativistic-energy limit¹¹

$$\psi^v \sim \sum_{\alpha, \kappa} V_{\alpha, \kappa}^v \begin{pmatrix} \cos[k_\alpha r + y \ln 2k_\alpha r - \frac{1}{2}(l+1)\pi + \delta^v] \\ -i \sin[k_\alpha r + y \ln 2k_\alpha r - \frac{1}{2}(l+1)\pi + \delta^v] \end{pmatrix} \varphi_{\alpha, \kappa}^v \quad (8)$$

The wave number k_α and the energy W_0 of the electron are given by energy conservation,

$$k_\alpha = W_\alpha / \hbar c = (E - E_{N, \alpha}) / \hbar c, \quad (9)$$

where E is the incident energy of the electron and $E_{N, \alpha}$ is the nuclear excitation energy. The logarithmic phase $y \ln 2k_\alpha r = Ze^2 / \hbar c \ln 2k_\alpha r$ comes from the static Coulomb field. The channel wave function is given by the nuclear wave function $|\alpha, J, J_z\rangle$ coupled with the spin-angular part¹⁵ of the solution of the Dirac equation $\chi_{\pm \kappa}^\mu$ to a total spin I :

$$\varphi_{\alpha, \kappa} = r^{-1} \sum_{\mu} \langle j, J, \mu, I - \mu | I, I \rangle \langle \alpha, J, I - \mu | \chi_{-\kappa}^\mu \rangle. \quad (10)$$

Here we have set $\langle I_z \rangle = I$, since the rotational invariance implies that the S matrix does not depend on $\langle I_z \rangle$.

The eigenchannel wave function (8) represents a superposition of standing waves with a common phase—the eigenphase—in all physical channels. We

¹⁵ M. E. Rose, *Relativistic Electron Theory* (Wiley-Interscience, Inc., New York, 1961).

can compute the eigenphase δ^v and the eigenvectors $V_{\alpha, \kappa}^v$, and thus the S matrix (5), by matching the solutions of the total Hamiltonian H to these standing waves. To achieve this, we introduce a cutoff radius¹⁶ a and evaluate there a set of boundary conditions, which the interior solutions of H have to meet. In the case of potential scattering, where $H_{\text{int}} \equiv 0$, these interior solutions are given by¹¹

$$\tilde{\Phi}_{\alpha, \kappa} \sim a^{-1/2} \times \begin{pmatrix} \cos[\tilde{k}_\alpha r + y \ln 2\tilde{k}_\alpha r - \frac{1}{2}(l+1)\pi + \tilde{\delta}_{\alpha, \kappa}^{\text{pot}}] \\ -i \sin[\tilde{k}_\alpha r + y \ln 2\tilde{k}_\alpha r - \frac{1}{2}(l+1)\pi + \tilde{\delta}_{\alpha, \kappa}^{\text{pot}}] \end{pmatrix} \varphi_{\alpha, \kappa} \quad (11)$$

in the asymptotic region; the normalization is in a sphere of radius α . We can obviously match these solutions to the standing waves (10) by continuing them into the outside region where $r > \alpha$, and get thereby

$$\tilde{k}_\alpha = k_\alpha \quad \text{and} \quad \delta^v = \tilde{\delta}_{\alpha, \kappa}^{\text{pot}} = \delta_{\alpha, \kappa}^{\text{pot}}. \quad (12)$$

Thus, the eigenphases are equal to the potential scattering phases in the physical channels. Now when H_{int} is included the various physical channels are coupled and the interior energies are no longer equal to

¹⁶ For our following calculations, we choose $a = 10^5$ fm. Since we deal with electron energies up to 250 MeV and angular momenta up to 27, the condition $ka \gg l(l+1)$ is always fulfilled, and it is thus justified to deal with asymptotic wave functions at the boundary radius. In principle, the choice of a has no influence on the S matrix in the EKT, as long as the range of H_{int} is smaller than a (note that the most critical r^{-1} term of the multipole expansion of the electromagnetic interaction is already included in H_0) and the nuclear wave functions guarantee channel orthogonality in the interior region. For the iteration procedure as developed below, however, it is convenient to choose a large a . On the other hand, this can lead to numerical difficulties in the evaluation of the transition matrix elements.

E as in (12), but are shifted by a certain amount (Figs. 1 and 2), and the eigenphases have to be shifted accordingly to yield the matching condition. Since one expects this shift to be small from a simple schematic-model calculation, the wave functions (11) serve as an excellent basis for the diagonalization of the total Hamiltonian in the interior region.¹⁷ Applying the matching condition to the basis set, we get

$$\tan[\tilde{k}_\alpha(\delta^\nu)a + y \ln 2\tilde{k}_\alpha(\delta^\nu)a + \tilde{\delta}_{\alpha,\kappa}^{\text{pot}}] = \tan(k_\alpha a + y \ln 2k_\alpha a + \delta^\nu) \quad (13)$$

or

$$\tilde{k}_\alpha(\delta^\nu)a + y \ln 2\tilde{k}_\alpha(\delta^\nu)a + \tilde{\delta}_{\alpha,\kappa}^{\text{pot}} = k_\alpha a + y \ln 2k_\alpha a + \delta^\nu + n\pi, \quad (14)$$

for the interior wave numbers $\tilde{k}_\alpha(\delta^\nu)$, which are a function of the still unknown eigenphases δ^ν . For the subsequent discussion, it is now important to notice that the potential scattering phases are only slowly varying functions of \tilde{k}_α . This is because we deal with incident electron energies E of $100 \leq E \leq 250$ MeV and are thus far-off resonances of the electron above the static potential (Fig. 1). Also, since the logarithm is a slowly varying function of \tilde{k}_α ($2\tilde{k}_\alpha a \approx 10^6$ for $E=100$

MeV and $a=10^5$ fm), we can cancel the logarithmic terms and drop the tilde above the potential scattering phase $\tilde{\delta}_{\alpha,\kappa}^{\text{pot}}$. Thus (14) becomes

$$\tilde{k}_\alpha(\delta^\nu) = k_\alpha + a^{-1}(\delta^\nu - \delta_{\alpha,\kappa}^{\text{pot}} + n\pi). \quad (15)$$

A necessary condition in going from (14) to (15) is that the excitation energies between the various states $|\alpha, J^\pm\rangle$ are not too high, because only then does the condition $|\delta^\nu - \delta_{\alpha,\kappa}^{\text{pot}}| \ll 1$, which guarantees that the \tilde{k}_α are close to the k_α , hold.¹⁸ We choose now a certain channel $\{c_0\} = \{\alpha_0, \kappa_0\}$ and make for all eigenphases the same zero-order ansatz

$$\delta^\nu = \delta_{c_0}^{\text{pot}} = \delta_{\alpha_0, \kappa_0}^{\text{pot}}. \quad (16)$$

With the help of Eqs. (9) and (15), we then get for the interior energies

$$\tilde{E}_{c,n} = E + (\hbar c/a)(\delta_{c_0}^{\text{pot}} - \delta_c^{\text{pot}} + n\pi), \quad (17)$$

where n is an additional radial quantum number. The diagonalization of the matrix of the total Hamiltonian¹⁹

$$\langle \tilde{\Phi}_{\alpha,\kappa,n} | H | \tilde{\Phi}_{\alpha',\kappa',n'} \rangle = \tilde{E}_{\alpha,\kappa,n} \delta_{\alpha,\kappa,n;\alpha',\kappa',n'} + \langle \Phi_{\alpha,\kappa,n} | H_{\text{int}} | \Phi_{\alpha',\kappa',n'} \rangle \quad (18)$$

is equivalent to the solution of the secular equation²⁰

$$a^{-1} \det \begin{pmatrix} \hbar c(\delta_{c_0}^{\text{pot}} - \delta_{c_1}^{\text{pot}} + n_1\pi) + \langle \Phi_{c_1,n_1} | H_{\text{int}} | \Phi_{c_1,n_1} \rangle & \cdots & \langle \Phi_{c_1,n_1} | H_{\text{int}} | \Phi_{c_M,n_M} \rangle \\ \cdots & \cdots & \cdots \\ \hbar c(\delta_{c_0}^{\text{pot}} - \delta_{c_M}^{\text{pot}} + n_M\pi) + \langle \Phi_{c_M,n_M} | H_{\text{int}} | \Phi_{c_M,n_M} \rangle & \cdots & \cdots \end{pmatrix} = \hat{E}^\nu - E, \quad (19)$$

where $M=N \times N'$, N being the number of physical channels which can be coupled to a total spin I , and N' the number of radial quantum numbers n of the basis set which are taken into account. The off-resonance argument leads again to the conclusion that the matrix elements on the left-hand side of (19) vary only slowly with the energy. The matching condition, i.e., the vanishing of the right-hand side of (19), can thus be fulfilled by subtracting the right-hand side from the entire equation, or, equivalently, by renormalizing the eigenphases:

$$\delta^\nu = \delta_{\alpha_0, \kappa_0}^{\text{pot}} + \Delta\delta^\nu = \delta_{\alpha_0, \kappa_0}^{\text{pot}} - (\hat{E}^\nu - E)(a/\hbar c). \quad (20)$$

A prescription has still to be given on the particular choice of the \hat{E}^ν in (19), because there are $M=N \times N'$ eigenvalues \hat{E}^ν but only N eigenchannels. The unperturbed energy levels $\tilde{E}_{\alpha,\kappa,n}$ [Eq. (17)] are ordered in multiplets for every radial quantum number n (Fig. 2), because the differences between the potential scattering phases are much smaller than π if the energy loss of the electron is not too large. Since the perturbation is small,

the perturbed energies \hat{E}^ν are arranged in a similar pattern of multiplets. To get the best values for the eigenphases, it is then convenient to take for the renormalization of the eigenphases (20) those \hat{E}^ν of the set which correspond to $n=0$ and which lie in the immediate vicinity of E , because then the renormalization will be smallest. In our actual calculation, we dropped the states with $n \neq 0$ from the beginning. Applying first-order perturbation theory to the interior stationary states (17), one sees that the ratio Q of the admixture coefficients of a state with $n=\pm 1$ and a state with $n=0$ is determined by the energy differences between these levels and the eigenchannel. These energy differences are proportional to the phase differences (17),

¹⁸ Typical values of $|\delta^\nu - \delta_{\alpha,\kappa}^{\text{pot}}|$ are 1.5×10^{-1} at $E=200$ MeV and an energy loss of 5 MeV (see Ref. 11). Therefore, $|\tilde{W}_\alpha - W_\alpha| = (\hbar c/a) \times 1.5 \times 10^{-1} \approx (3 \times 10 \text{ fm}) a^{-1} \text{ MeV}$. This corresponds to $|\delta_{\alpha,\kappa}^{\text{pot}} - \delta_{\alpha,\kappa}^{\text{pot}}| \approx 3 \times 10^{-1} a^{-1}$, where a is in fm. The potential scattering phases themselves can, for numerical reasons, only be determined up to an accuracy of about 5×10^{-6} .

¹⁹ Although the interior radial wave functions of the electron are not orthogonal, because they obey different boundary conditions in different channels $\{\alpha\}$ [Eq. (15)], the orthogonality of the wave functions $\Phi_{\alpha,\kappa,n}$ is guaranteed by the orthogonality of the channel wave functions. Because $|\tilde{W}_\alpha - W_\alpha| \ll 1$ (see Ref. 18), we also dropped the tilde in the matrix elements of H_{int} .

²⁰ A factor a^{-1} can be taken in front of the interaction matrix elements because of the normalization of the interior wave functions of the electron.

¹⁷ Because of the large incident energy of the electron, we can neglect the electronic bound states, which must be taken together with the states $\alpha, \tilde{\Phi}_\alpha$ to form a complete set.

so that we get (Fig. 2)

$$Q = \max |\delta_{\alpha, \kappa}^{\text{pot}} - \delta_{\alpha', \kappa'}^{\text{pot}}| / \pi \approx 5\%. \quad (21)$$

Because of the weak coupling, the admixture coefficients of the states which are taken into account are very small themselves, namely, of the order 5×10^{-2} . Thus the neglected states would give contributions of the order of 0.25% to the S matrix. In reality, however, the error will be even smaller, since one expects the contribution of states with opposite sign of n to cancel.

With the eigenphases δ^ν and the eigenvectors $V_{\alpha, \kappa}^\nu$, which are given by the diagonalization of the S matrix, we can compute the S matrix

$$S_{\alpha, \kappa; \alpha', \kappa'}^{I, \pi} = \sum_\nu V_{\alpha, \kappa}^{I, \pi, \nu} \exp(2i\delta^{I, \pi, \nu}) V_{\alpha', \kappa'}^{I, \pi, \nu}. \quad (22)$$

The differential cross section for the excitation of a nuclear state $|\alpha', J'\rangle$ from a state $|\alpha, J\rangle$ is then given by¹¹

$$\begin{aligned} \left(\frac{d\sigma}{d\Omega}\right)_{\alpha \rightarrow \alpha'} &= \frac{\pi}{k_\alpha^2} \frac{1}{2(2J+1)} \sum_{\nu, \tau, \nu', \tau'} \left| \sum_{I, M, \kappa, \kappa'} i^{l-l'} (2l+1)^{1/2} \right. \\ &\quad \times (l, \frac{1}{2}, 0, \tau | j, \tau) (j, J, \tau, \nu | I, M) \\ &\quad \times (l', \frac{1}{2}, \mu' - \tau', \tau' | j', \mu') (j', J', \mu', \nu' | I, M) \\ &\quad \left. \times (S_{\alpha', J', \kappa'; \alpha, J, \kappa}^{I, \pi} - \delta_{\alpha', J', \kappa'; \alpha, J, \kappa}) Y_{l', \mu' - \tau'}(\hat{p}_{\alpha'}) \right|^2, \quad (23) \end{aligned}$$

where the incident beam travels in the z direction, and $\hat{p}_{\alpha'}$ is the direction of the scattered electron. The form factor is defined as

$$|F|^2 = (d\sigma/d\Omega) / \sigma_{\text{Mott}}, \quad (24)$$

where the Mott cross section is given in the high-relativistic-energy limit by (θ is the scattering angle)

$$\sigma_{\text{Mott}} = 4(Ze^2)^2 E^2 \cos^2(\frac{1}{2}\theta) / (2E \sin^2\theta)^4. \quad (25)$$

As initial values for the one-step iteration procedure for the S matrix we need the potential scattering phases $\delta_{\alpha, \kappa}^{\text{pot}}$ and the matrix elements of the interaction Hamiltonian H_{int} . These quantities are computed with a code previously used for DWBA calculations.²¹⁻²³ Because the higher-order effects show up in differences between the DWBA form factors F_D^2 and the EKT form factors F_E^2 , it is useful to make a DWBA calculation parallel to the EKT calculation. For this we have only to replace the S -matrix elements in (23) by their first-order DWBA values. These are

$$\tilde{S}_{\alpha, J, \kappa; \alpha, J, \kappa}^{I, \pi} = \exp(2i\delta_{\alpha, \kappa}^{\text{pot}}), \quad (26)$$

for elastic scattering, and

$$\begin{aligned} \tilde{S}_{\alpha', J', \kappa'; \alpha, J, \kappa}^{I, \pi} &= -(2ia/\hbar c) \exp(i(\delta_{\alpha, \kappa}^{\text{pot}} + \delta_{\alpha', \kappa'}^{\text{pot}})) \\ &\quad \times \langle \Phi_{\alpha', \kappa', 0} | H_{\text{int}} | \Phi_{\alpha, \kappa, 0} \rangle. \quad (27) \end{aligned}$$

With these expressions introduced into Eq. (23) for the differential cross section, one gets, after some recoupling, the conventional formulas for the elastic¹⁵ and the inelastic²¹⁻²³ differential cross section.

III. CLOSED FORMULA FOR S MATRIX

Although we will use in the following calculations the above-described diagonalization procedure, in which explicit reference is made to the intermediate states, it is very convenient for the interpretation of our results to apply the conventional perturbation theory to the states (17) and to give the S matrix (22) as an expansion in orders of H_{int} .

In zeroth order, the physical channels and the eigenchannels are identical, and we have

$$\begin{aligned} \{\nu\} &= \{c_0\}, \\ V_c^\nu &= V_c^{c_0} = \Delta_{c, c_0}, \\ \delta^\nu &= \delta^{c_0} = \delta_{c_0}^{\text{pot}}, \end{aligned} \quad (28)$$

where we denoted the Kronecker δ by Δ in order to avoid confusion with the phases δ . Introduction of (28) in (22) gives the S matrix in zeroth order:

$$S_{cc'} = \exp(2i\delta_c^{\text{pot}}) \Delta_{cc'}, \quad (29)$$

which is identical with (26).

In first order, we have for the admixture coefficients

$$\begin{aligned} V_c^{c_0} &= H_{cc_0} / (\tilde{E}_{c_0} - \tilde{E}_c), \quad c \neq c_0 \\ &= 1, \quad c = c_0 \end{aligned} \quad (30)$$

with

$$H_{cc_0} = \langle \Phi_{c, 0} | H_{\text{int}} | \Phi_{c_0, 0} \rangle,$$

and the eigenphases, according to (20), are

$$\begin{aligned} \delta^{c_0} &= \delta_{c_0}^{\text{pot}} - (\tilde{E}_{c_0} - E) a / \hbar c \\ &= \delta_{c_0}^{\text{pot}} - (\tilde{E}_{c_0} - E + H_{c_0 c_0}) a / \hbar c \\ &= \delta_{c_0}^{\text{pot}} - (a / \hbar c) H_{c_0 c_0}, \end{aligned} \quad (31)$$

because by construction $\tilde{E}_{c_0} = E$. Then S is, up to term linear in H_{int} ,

$$\begin{aligned} S_{cc'} &= \sum_{c_0} V_c^{c_0} \exp(2i\delta^{c_0}) V_{c'}^{c_0} \\ &= \exp 2i[\delta_c^{\text{pot}} - (a/\hbar c) H_{cc}] \Delta_{cc'} \\ &\quad + V_{c'}^{c'} \exp(2i\delta_c^{\text{pot}}) + V_c^{c'} \exp(2i\delta_{c'}^{\text{pot}}). \end{aligned} \quad (32)$$

We have then for the diagonal elements

$$S_{cc} = \exp(2i\delta_c^{\text{pot}}) [1 - 2i(a/\hbar c) H_{cc}], \quad (33)$$

i.e., an additional term, which becomes important if the nuclear state $\{c\}$ has, for example, a static quadrupole moment. For the off-diagonal elements we note that [from (17) and (30)]

$$V_{c'}^{c'} = -V_c^{c'} = \frac{H_{c'e}}{\tilde{E}_e - \tilde{E}_{c'}} = \frac{a}{\hbar c} \frac{H_{c'e}}{\delta_{c'}^{\text{pot}} - \delta_c^{\text{pot}}}. \quad (34)$$

²¹ D. Drechsel, Nucl. Phys. **78**, 465 (1966); Z. Physik **192**, 81 (1966).

²² D. Drechsel and C. Toepffer, Nucl. Phys. **A100**, 161 (1967).

²³ C. Toepffer and D. Drechsel, Z. Physik **210**, 423 (1968).

Then we have

$$S_{cc'} = \exp i(\delta_{c'}^{\text{pot}} + \delta_c^{\text{pot}}) \left[\exp i(\delta_c^{\text{pot}} - \delta_{c'}^{\text{pot}}) - \exp i(\delta_{c'}^{\text{pot}} - \delta_c^{\text{pot}}) \right] (a/\hbar c) H_{c'e'} / (\delta_{c'}^{\text{pot}} - \delta_c^{\text{pot}}). \quad (35)$$

Under the condition that the energy loss of the electron is not too high, so that $|\delta_{c'}^{\text{pot}} - \delta_c^{\text{pot}}| \ll 1$,²⁴ one can expand the exponentials in the second factor, and one gets

$$S_{cc'} = S_{c'e} = -2i(a/\hbar c) \exp i(\delta_c^{\text{pot}} + \delta_{c'}^{\text{pot}}) H_{c'e}, \quad (36)$$

which corresponds to (27).

To get S_{cc} up to terms quadratic in H_{int} we need the second-order admixture coefficients

$$\begin{aligned} V_{c'c_0} &= 1 - \frac{1}{2} \sum_{c'} |H_{c'e}|^2 / (\tilde{E}_c - \tilde{E}_{c'}), & c = c_0 \\ &= H_{cc_0} / (\tilde{E}_{c_0} - \tilde{E}_c) + (\text{second-order terms}), & c \neq c_0 \end{aligned} \quad (37)$$

and the second-order energy shift

$$\tilde{E}_{c_0} - E = H_{cc_0} + \sum_{c'} \frac{|H_{c'e}|^2}{\tilde{E}_{c_0} - \tilde{E}_{c'}}. \quad (38)$$

We have then for the diagonal S -matrix elements

$$\begin{aligned} S_{cc} &= \left(1 - \frac{1}{2} \sum_{c'} \frac{|H_{c'e}|^2}{(\tilde{E}_c - \tilde{E}_{c'})^2} \right) \\ &\times \exp 2i \left(\delta_c^{\text{pot}} - \frac{a}{\hbar c} H_{cc} - \frac{a}{\hbar c} \sum_{c'} \frac{|H_{c'e}|^2}{\tilde{E}_c - \tilde{E}_{c'}} \right) \\ &\times \left(1 - \frac{1}{2} \sum_{c'} \frac{|H_{c'e}|^2}{(\tilde{E}_c - \tilde{E}_{c'})^2} \right) + \sum_{c_0} \frac{H_{cc_0}}{\tilde{E}_{c_0} - \tilde{E}_c} \\ &\times \exp(2i\delta_{c_0}^{\text{pot}}) \frac{H_{cc_0}}{\tilde{E}_{c_0} - \tilde{E}_c} \quad (39) \\ &= \exp(2i\delta_c^{\text{pot}}) \left[1 - 2i \frac{a}{\hbar c} H_{cc} - 2i \frac{a}{\hbar c} \sum_{c'} \frac{|H_{c'e}|^2}{\tilde{E}_c - \tilde{E}_{c'}} \right. \\ &\left. - 2 \left(\frac{a}{\hbar c} \right)^2 |H_{cc}|^2 - \sum_{c'} \frac{|H_{c'e}|^2}{(\tilde{E}_c - \tilde{E}_{c'})^2} + \sum_{c'} \frac{H_{cc'}}{\tilde{E}_{c'} - \tilde{E}_c} \right] \\ &\times \exp 2i(\delta_{c'}^{\text{pot}} - \delta_c^{\text{pot}}) \frac{H_{cc'}}{\tilde{E}_{c'} - \tilde{E}_c}. \quad (40) \end{aligned}$$

If one expands the exponential in the last term up to quadratic terms, the third and fifth terms of the bracket cancel against the absolute and linear terms of the expansion, and one is left with

$$S_{cc} = \exp(2i\delta_c^{\text{pot}}) \left[1 - 2i \frac{a}{\hbar c} H_{cc} - 2 \left(\frac{a}{\hbar c} \right)^2 \sum_{c'} |H_{c'e}|^2 \right]. \quad (41)$$

²⁴ This condition has already been used in the derivation of the simplified matching condition (15).

Neglecting the retardation in H_{int} and the energy loss of the electron in a virtual transition, so that $k_\alpha \equiv k$, we get, by applying the closure relation²⁵ to the radial nuclear wave functions $f_{\alpha,J}$,

$$S_{cc} = \exp(2i\delta_c^{\text{pot}}) \left[1 - 2i \frac{a}{\hbar c} H_{cc} - 2 \left(\frac{a}{\hbar c} \right)^2 \sum_{J',\kappa'} \langle f_{\alpha,J} | g_{J,\kappa} | H_{\text{int}} | g_{J',\kappa'} \rangle \langle g_{J',\kappa'} | H_{\text{int}} | g_{J,\kappa} \rangle f_{\alpha,J} \right], \quad (42)$$

where the functions $f_{\alpha,J}$ and $g_{J,\kappa}$ are defined in terms of the total interior wave function (10) and (11) by

$$\begin{aligned} \Phi_{\alpha,\kappa,0} &= a^{-1/2} \begin{pmatrix} \cos[kr + y \ln 2kr - \frac{1}{2}(l+1)\pi + \delta_c^{\text{pot}}] \\ -i \sin[kr + y \ln 2kr - \frac{1}{2}(l+1)\pi + \delta_c^{\text{pot}}] \end{pmatrix} \\ &\times r^{-1} f_{\alpha,J} \sum_{\mu} (j, J, \mu, I - \mu | I, I) | J, I - \mu \rangle \begin{pmatrix} \chi_{\kappa}^{\mu} \\ \chi_{-\kappa}^{-\mu} \end{pmatrix} \\ &= g_{J,\kappa} f_{\alpha,J}. \quad (43) \end{aligned}$$

Before we interpret (42), let us recall the conditions on which the iteration procedure is based: We have to deal with large incident electron energies and a large cutoff radius a . If the energy loss of the electron in a virtual excitation is not too large, so that the phase differences are small, we can drop the tilde above the potential scattering phases (15) and the interior wave functions (18) and also neglect the states with $n \neq 0$. Also, because the coupling between the channels is weak, we can make the same ansatz¹⁶ for all eigenphases, which means that we work in the *same* Hilbert space when evaluating different eigenchannels. We find, moreover, that only one iteration is necessary to get highly accurate S -matrix elements. The same conditions are important for the evaluation of (42). In order to compare these results with the conventional ones [Eqs. (26) and (27)], the tilde on the potential scattering phases and the wave functions must be dropped, and explicit use must be made of the small phase differences. However, there is no need to distinguish between interior and exterior admixture coefficients (as in the case of nuclear reactions,⁹) because we use only the states with $n=0$ and construct all eigenchannels with the same Hilbert space.

Although we made a restriction on the energy loss of the electron in deriving (41), we may use the completeness relation in going from (41) to (42), because it seems quite unreasonable that states with an energy comparable to the incident electron energy (only then do the phase differences become of order 1) are important as intermediate states. Should, for example,

²⁵ We thank Professor H. Marschall for clarifying discussions about this point.

virtual pion production play a role in the scattering of 250-MeV electrons?

We can therefore state that the S matrix depends on the energies of the intermediate states only through the interaction matrix elements, because there are no explicitly energy-dependent terms—such as energy denominators—in (41) and (42). Equation (41) states that the second-order contribution to the S matrix is the sum of the contributions of the particular intermediate states, and therefore Eqs. (41) and (42) open the possibility of using sum rules for the calculation of higher-order effects instead of making explicit reference to intermediate states.

In the following calculations, we shall use the iteration procedure for the construction of the S matrix, as outlined in Sec. II, to show that our explicit results are in accordance with the conclusions we can draw from the above closed forms (41) and (42) for the S matrix.

IV. NUCLEAR MODEL

The interaction between the electron and the nucleus is given by

$$H_{\text{int}} = \int d\tau_N [\rho_N \Phi_e^{\text{ret}}(\mathbf{r}_N) - (1/c) \mathbf{j}_N \mathbf{A}_e^{\text{ret}}(\mathbf{r}_N)], \quad (44)$$

where Φ_e^{ret} and $\mathbf{A}_e^{\text{ret}}$ are the retarded potentials of the electron at the nucleus. The matrix elements of H_{int} are computed using the multipole expansion of H_{int} ^{26,27} and inserting the wave functions Φ [of which the asymptotic behavior was given in (11)]. Neglecting the retardation²⁸ and the contributions from the nuclear current and magnetization, we have for the interaction matrix elements¹⁰

$$\begin{aligned} \langle \Phi_{\alpha', \kappa'} | H_{\text{int}} | \Phi_{\alpha, \kappa} \rangle &= -2\pi^{1/2} (-1)^{1-J'-I+j+j'+1/2} \\ &\quad \times [(2j'+1)(2j+1)]^{1/2} \sum_{\lambda} (2\lambda+1)^{-1/2} \\ &\quad \times \begin{Bmatrix} j' & j & \lambda \\ J & J' & I \end{Bmatrix} \begin{pmatrix} j' & \lambda & j \\ \frac{1}{2} & 0 & -\frac{1}{2} \end{pmatrix} \frac{1}{2} [1 + (-1)^{\nu'+\lambda+l}] \\ &\quad \times \int_0^a dr_e r_e^2 (f_{\alpha', \kappa'} f_{\alpha, \kappa} + g_{\alpha', \kappa'} g_{\alpha, \kappa}) J_{\alpha, J \rightarrow \alpha', J'}^{(\lambda)}(r_e), \end{aligned} \quad (45)$$

where

$$\begin{aligned} J_{\alpha, J \rightarrow \alpha', J'}^{(\lambda)} &= e \int_0^a dr_N r_N^2 \int d\Omega_N \frac{r_{<}^{\lambda}}{r_{>}^{\lambda+1}} \\ &\quad \times \langle \alpha', J' | \rho_N Y_{\lambda}(\Omega_N) | \alpha, J \rangle \end{aligned} \quad (46)$$

²⁶ F. Scheck, Nucl. Phys. **77**, 577 (1965).

²⁷ L. C. Biedenharn and P. J. Brussaard, *Coulomb Excitation* (Clarendon Press, Oxford, 1965).

²⁸ Consistently, one must then also neglect the energy loss in the transition matrix elements. This means that there is no dependence on the energy of the intermediate states at all in (19) and (42). Moreover, one must also neglect the energy loss in the phase differences in (19) and (42) in order to compare $|F|_E^2$ and $|F|_p^2$ consistently for inelastic scattering. This was not done for $|F|_E^2$ in a previous publication (Ref. 12), and therefore the dispersion effects for inelastic scattering turned out to be somewhat too large there.

is the transition potential. The radial wave functions f and g of the electron are solutions of the radial Dirac equation¹⁵:

$$\frac{df}{dr} = \frac{\kappa-1}{r} f - \frac{W-V(r)}{\hbar c} g, \quad (47)$$

$$\frac{dg}{dr} = \frac{W-V(r)}{\hbar c} f - \frac{\kappa+1}{r} g.$$

These coupled equations are integrated numerically up to a certain radius R_{max} and the resulting wave functions f and g are inserted in (45), where the integrals can then be computed up to R_{max} . For $R_{\text{max}} < r_e < a$ we use the asymptotic expansions for f and g up to terms of the order $O(k_e r)^{-2}$, with which the remaining integral can be calculated analytically.²⁹

The static potential $V(\mathbf{r})$ is the solution of the Poisson equation

$$\nabla^2 V(\mathbf{r}) = 4\pi e \rho_{\text{st}}(\mathbf{r}), \quad (48)$$

where $\rho_{\text{st}}(\mathbf{r})$ is the model-dependent charge density of the nucleus. In our calculations we will use a spherical Fermi distribution³⁰

$$\rho_{\text{st}}(r) = Z e \rho_0(r), \quad (49)$$

$$\rho_0(r) = \frac{3/4\pi c^3}{1 + (\pi a/c)^2 - 6W_3(0, a/c)} \frac{1}{1 + \exp[(r-c)/a]}, \quad (50)$$

and

$$a = t/4 \ln 3. \quad (51)$$

c is the half-density radius, t is the 90–10% surface thickness, and $W_3(0, a/c)$ is a function defined in Ref. 30.

In order to calculate the interaction matrix elements, we further have to specify the excited states of the nucleus. In the spherical medium-heavy even-even nuclei, the nuclear spectrum can be described fairly well by the collective model with two different kinds of modes: (a) $T=0$ vibrational modes for the low-energy states, and (b) $T=1$ giant-resonance modes for the high-energy ($E \geq 15$ MeV) states. For the vibrational states we use the harmonic-vibrator model in which the charge-density operator is given by

$$\rho_N(\mathbf{r}) = \rho_{\text{st}}(r) - r \frac{d\rho_{\text{st}}}{dr} \sum_{\lambda} (2\lambda+1)^{1/2} [\alpha^{(\lambda)} \times Y^{(\lambda)}]^{(0)}, \quad (52)$$

to first order in the collective coordinate $\alpha_{\mu}^{(\lambda)}$. To in-

²⁹ This is not possible if the transverse part of the interaction is included in (45). One must then choose a smaller cutoff radius a with $a = R_{\text{max}}$.

³⁰ T. Schucan, Nucl. Phys. **61**, 417 (1965).

clude second-order terms we extend (52) by^{31,32}

$$\rho_N(r) = \rho_{st}(r) - r \frac{d\rho_{st}}{dr} \sum_{\lambda} (2\lambda+1)^{1/2} [\alpha^{[\lambda]} \times Y^{[\lambda]}]^{[0]} + r^2 \frac{d^2\rho_{st}}{dr^2} \left\{ \sum_{\lambda} (2\lambda+1)^{1/2} [\alpha^{[\lambda]} \times Y^{[\lambda]}]^{[0]} \right\}^2. \quad (53)$$

The collective coordinates $\alpha_{\mu}^{[\lambda]}$ can be written in terms of creation and annihilation operators for surface phonons:

$$\alpha_{\mu}^{[\lambda]} = \beta_{\lambda} (2\lambda+1)^{-1/2} [\beta_{\mu}^{[\lambda]\dagger} + (-)^{\mu} \beta_{-\mu}^{[\lambda]}]. \quad (54)$$

Here the effective deformation β_{λ} is related to the mass and force constants B_{λ} and C_{λ} in the Hamiltonian of the harmonic vibrator by

$$\beta_{\lambda} = \left(\frac{(2\lambda+1)\hbar}{2(B_{\lambda}C_{\lambda})^{1/2}} \right)^{1/2} = \left(\frac{(2\lambda+1)\hbar\omega_{\lambda}}{2C_{\lambda}} \right)^{1/2}, \quad (55)$$

where $\omega_{\lambda} = (C_{\lambda}/B_{\lambda})^{1/2}$ is the oscillator frequency of multipolarity λ . We can now calculate the transition potentials between all vibrational states including the ground state, which is by assumption a 0^+ state.

In Eq. (53) for the charge-density operator the parameters of the higher terms are fully determined by the parameters of this static charge distribution. In order to fit the experimental inelastic cross sections, it is convenient to loosen this restriction by allowing for different parameters in the derivations of the charge distribution. Then we have

$$\rho_N(\mathbf{r}) = \rho_{st}(r) - Zer \frac{d\rho_0}{dr} \sum_{\lambda} \frac{N_{\lambda}}{\beta_{\lambda}} (2\lambda+1) \times [\alpha^{[\lambda]} \times Y^{[\lambda]}]^{[0]} + Zer^2 \frac{d^2\rho_0}{dr^2} \sum_{\lambda} \left(\frac{N_{\lambda}}{\beta_{\lambda}} (2\lambda+1) \times [\alpha^{[\lambda]} \times Y^{[\lambda]}]^{[0]} \right)^2 \quad (56)$$

with³³

$$\rho_0(r) = \frac{3/4\pi c_{tr}^3}{1 + (\pi a_{tr}/c_{tr})^2 - 6W_8(0, a_{tr}/c_{tr})} \times \frac{1}{1 + \exp[(r - c_{tr})/a_{tr}]}. \quad (57)$$

The strength constants N_{λ} can be adjusted to give the correct reduced transition probability, which is defined

as

$$B(E\lambda, 0^+ \rightarrow \lambda^+) = \left| \left\langle \beta^{[\lambda]\dagger} \left\| \int dr r^{\lambda} \rho_N(\mathbf{r}) Y_{\lambda} \right\| 0 \right\rangle \right|^2 = Z^2 e^2 N_{\lambda}^2 (2\lambda+1) I_{\lambda}^2, \quad (58)$$

with

$$I_{\lambda} = \int_0^{\infty} r^{\lambda+3} \frac{d\rho_0}{dr} dr. \quad (59)$$

The reduced transition probability is in turn related, up to first order, to the effective deformation β_{λ} by³⁴

$$B(E\lambda, 0^+ \rightarrow \lambda^+) = [3/(4\pi) ZeR_0^{\lambda}]^2 \beta_{\lambda}^2, \quad (60)$$

with $R_0 = 1.2A^{1/3}$ fm.

The transition potential (46) is then, upon insertion of (56), up to first-order terms,

$$J_{0^+ \rightarrow \lambda^+}^{(\lambda)} = -Ze^2 N_{\lambda} (2\lambda+1)^{1/2} \times \left(r_e^{-1-\lambda} \int_0^{r_e} dr r^{\lambda+3} \frac{d\rho_0}{dr} + r_e^{\lambda} \int_{r_e}^{\infty} dr r^{-\lambda+2} \frac{d\rho_0}{dr} \right). \quad (61)$$

For the giant resonances we use the dynamic collective model due to Danos, Greiner, and co-workers^{35,36}. The giant dipole mode consists of an out-of-phase motion of protons and neutrons, for which the symmetry term of the Bethe-Weizsäcker formula gives the restoring potential. Because of the change of the radii of the principal nuclear axes in a vibration, the giant-resonance modes are coupled to the vibrational modes, which we discussed earlier. This coupling leads to a splitting of the giant-resonance states. It has been shown that the main peaks in the giant-resonance region are 1^- states, where dipole phonons d^{\dagger} and quadrupole surface phonons β^{\dagger} are coupled:

$$| \alpha, 1^- \rangle = p_{\alpha} d^{\dagger} + q_{\alpha} [d^{\dagger} \times \beta^{\dagger}]^{[1^-]} + \text{higher terms}. \quad (62)$$

In the charge operator (56) a term must be added which describes this mode. The transition potential for a dipole transition into such a state is given by¹⁶

$$J_{\alpha, J \rightarrow \alpha', 1^-}^{(1)} = e^2 S^{(0)} \times \langle \alpha', 1^- | (d^{\dagger} + d) + S_{ad} [(d^{\dagger} + d) \times (\beta^{\dagger} + \beta)]^{[1^-]} | \alpha, J \rangle, \quad (63)$$

where

$$S_{ad} = -S_0^{(1)} \beta_2 / \sqrt{2} \quad (64)$$

and $S^{(0)}$ and $S_0^{(1)}$ are given in Ref. 16.

³¹ L. J. Tassie, Australian J. Phys. **9**, 407 (1965).

³² A consistent derivation of the nuclear charge-density operator [D. Drechsel, Z. Physik **181**, 542 (1964)], starting from a static uniform charge distribution, gives a first-order term with a radial dependence $\sim d\rho_{st}/dr$ and two second-order terms with a radial dependence $d^2\rho_{st}/dr^2$ and $d\rho_{st}/dr$, respectively. All these expansions of $\rho_N(\mathbf{r})$ have in common that the resulting transition densities have a peak of a width $\approx t$ at the nuclear radius.

³³ In the following calculations, however, we always use $c_{tr} = c$ and $a_{tr} = a$.

³⁴ O. Nathan and S. G. Nilsson, in *Alpha-, Beta- and Gamma-Ray Spectroscopy*, edited by Kai Siegbahn (North-Holland Publishing Co., Amsterdam, 1965), Chap. X.

³⁵ H. J. Weber, M. G. Huber, and W. Greiner, Z. Physik **192**, 182 (1966); **192**, 223 (1966); M. G. Huber, H. J. Weber, M. Danos, and W. Greiner, Phys. Rev. **155**, 1073 (1967).

³⁶ The properties of the dynamic collective model are also discussed in the review articles by M. G. Huber, Am. J. Phys. **35**, 685 (1967); H. Arenhövel and W. Greiner, in *Progress in Nuclear Physics*, edited by D. M. Brink and J. Mulvey (Pergamon Press, Ltd., Oxford, 1968), Vol. 10.

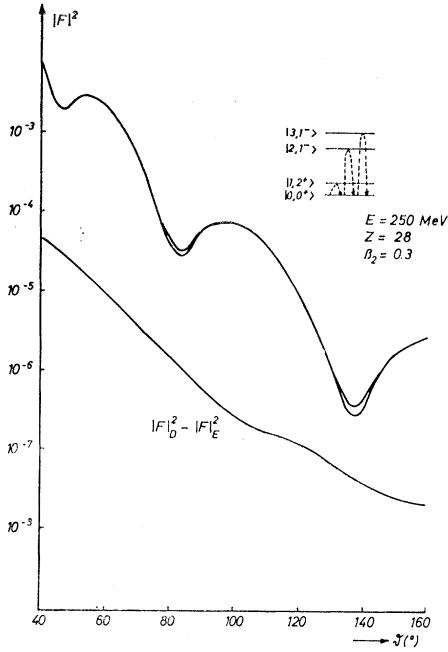


FIG. 3. Elastic form factors $|F|_{D^2}$ (DWBA) and $|F|_{E^2}$ (EKT) for $E=250$ MeV, Ni^{58} , and $\beta_2=0.3$. The wave functions of the intermediate states are $|1, 2^+\rangle = \beta^\dagger |0\rangle$, $|2, 1^-\rangle = d^\dagger |0\rangle$, and $|3, 1^-\rangle = [d^\dagger \times \beta^\dagger]^{(1-)} |0\rangle$. The broken lines in the nuclear spectrum represent the major virtual transition modes.

We will first consider in our calculations the ground-state with

$$|\alpha, J\rangle = |0, 0^+\rangle = |0\rangle, \quad (65)$$

and, in addition, a vibrational 2^+ state with

$$|\alpha, J\rangle = |1, 2^+\rangle = \beta^\dagger |0\rangle, \quad (66)$$

and two 1^- giant-resonance states with

$$|\alpha, J\rangle = |2, 1^-\rangle = (p_2 d^\dagger + q_2 [d^\dagger \times \beta^\dagger]^{(1-)} |0\rangle \quad (67)$$

and

$$|\alpha, J\rangle = |3, 1^-\rangle = (p_3 d^\dagger + q_3 [d^\dagger \times \beta^\dagger]^{(1-)} |0\rangle, \quad (68)$$

where in the last two wave functions the pairs $\{p_2, q_2\}$ and $\{p_3, q_3\}$ must be orthonormal. We have then to consider the following transition potentials³⁷ for the construction of the matrix (19):

$$J_{0,0^+ \rightarrow 1,2^+}^{(2)} = -Ze^2 N_2 (\sqrt{5}) \times \left(r_e^{-3} \int_0^{r_e} dr r^5 \frac{d\rho_0}{dr} + r_e^2 \int_{r_e}^a dr \frac{d\rho_0}{dr} \right), \quad (69)$$

$$J_{2,1^+ \rightarrow 3,1^-}^{(2)} = -Ze^2 N_2 \sqrt{3} (p_2 q_3 + q_2 p_3) \times \left(r_e^{-3} \int_0^{r_e} dr r^5 \frac{d\rho_0}{dr} + r_e^2 \int_{r_e}^a dr \frac{d\rho_0}{dr} \right),$$

³⁷ We neglect the octupole potentials $J_{1,2^+ \rightarrow \alpha,1^-}^{(3)}$, the monopole transition potentials between the 1^- states, and the reorientation in the 1^- states. The latter two transition potentials result from the two-surface-phonon terms in ρ_N .

from (61); and

$$\begin{aligned} J_{0,0^+ \rightarrow 2,1^-}^{(1)} &= e^2 \sqrt{3} S^{(0)} (p_2 + q_2 S_{ad}), \\ J_{0,0^+ \rightarrow 3,1^-}^{(1)} &= e^2 \sqrt{3} S^{(0)} (p_3 + q_3 S_{ad}), \\ J_{1,2^+ \rightarrow 2,1^-}^{(1)} &= e^2 \sqrt{3} S^{(0)} (q_2 + p_2 S_{ad}), \\ J_{1,2^+ \rightarrow 3,1^-}^{(1)} &= e^2 \sqrt{3} S^{(0)} (q_3 + p_3 S_{ad}), \end{aligned} \quad (70)$$

from (63).

V. DISPERSION EFFECTS IN ELASTIC SCATTERING

Unless otherwise specified, we use for our following calculations a nucleus with $Z=28$, $A=58$ (Ni^{58}), which has a Fermi-type static charge distribution with parameters $c=4.28$ fm and $t=2.49$ fm; the effective deformation is taken to be $\beta_2=0.3$, which corresponds to $B(E2, 0^+ \rightarrow 2^+) = 1872 e^2 \text{ fm}^4$ [see Eq. (60)]. The nuclear spectrum is shown in Fig. 3, which also shows the form factors $|F|_{D^2}$ and $|F|_{E^2}$ for elastic scattering of 250-MeV electrons and their absolute difference which is caused by virtual excitations to intermediate states.

In the following we will call the relative quantity $(|F|_{D^2} - |F|_{E^2})/|F|_{D^2}$ the "dispersion effect" and discuss its properties.

A. Dependence on Intermediate States and Virtual Transition Potentials

We repeated the calculation which led to Fig. 3 for $E=225$ MeV in three ways: (1) keeping only the 2^+ intermediate state, (2) keeping only the 1^- states, and (3) keeping all three intermediate states. The corresponding dispersion effects are shown in Table I near the three minima of the elastic cross section. The total effect is always the sum of those with different virtual excitation modes, but the dispersion effect resulting from a virtual excitation to the 1^- states has a different angular dependence from that resulting from a virtual excitation into the 2^+ state. The former gives the major contribution at small angles, the latter at back-

TABLE I. Dispersion effect in elastic scattering for $E=225$ MeV, $Z=28$, $\beta_2=0.3$, at angles near the minima of the first-order form factor $|F|_{D^2}$, with various possible intermediate states in the head line. The wave functions of the giant-resonance states are $|2, 1^-\rangle = (\frac{1}{2}\sqrt{3}d^\dagger + \frac{1}{2}[d^\dagger \times \beta^\dagger]^{(1-)} |0\rangle$ and $|3, 1^-\rangle = (-\frac{1}{2}d^\dagger + \frac{1}{2}\sqrt{3}[d^\dagger \times \beta^\dagger]^{(1-)} |0\rangle$.

Intermediate states (deg)	$ 1, 2^+\rangle$ (%)	$ 2, 1^-\rangle$ $ 3, 1^-\rangle$ (%)	$ 1, 2^+\rangle$ $ 2, 1^-\rangle$ $ 3, 1^-\rangle$ (%)
$\theta=50$	<0.1	1.5	1.3
$\theta=95$	2.3	2.4	4.7
$\theta=172$	12.3	≈ 0.1	12.4

ward angles.³⁸ To clarify this, we write Eqs. (23) and (26) in terms of the form factors:

$$|F|_{E^2} \sim \left| \sum_I f(I, \theta) (S_{\alpha, J, \kappa; \alpha', J', \kappa'} I - 1) \right|^2 \quad (71)$$

and

$$|F|_{D^2} \sim \left| \sum_I f(I, \theta) (\tilde{S}_{\alpha, J, \kappa; \alpha', J', \kappa'} I - 1) \right|^2. \quad (72)$$

These formulas differ *only* in the S -matrix elements; thus, writing

$$\Delta S^I = \tilde{S}^I - S^I, \quad (73)$$

we have for the dispersion effect in matrix notation

$$\frac{|F|_{D^2} - |F|_{E^2}}{|F|_{D^2}} \sim \frac{\sum_{I, I'} \text{Re}[f(I, \theta) f^*(I', \theta) (\tilde{S}^I - 1) \Delta S^{I' *}]}{\left| \sum_I f(I, \theta) (\tilde{S}^I - 1) \right|^2} \quad (74)$$

Now, by comparison with (26), one finds that ΔS^I is given simply by the last term in (41) and (42)³⁹:

$$\Delta S^I = \exp(2i\delta_I^{\text{pot}}) \left[-2 \left(\frac{a}{\hbar c} \right)^2 \sum_{c'} |H_{cc'}|^2 \right], \quad (75)$$

i.e., ΔS^I is a complex number, of which the argument $2i\delta_I^{\text{pot}}$ is independent of the intermediate states; its absolute value, however, is, the sum of the contributions of the virtual transitions to the different intermediate states. Now in the final sums (71) and (72) for the form factors, the S -matrix elements are added coherently, and therefore dispersion effect depends on the scattering angle.

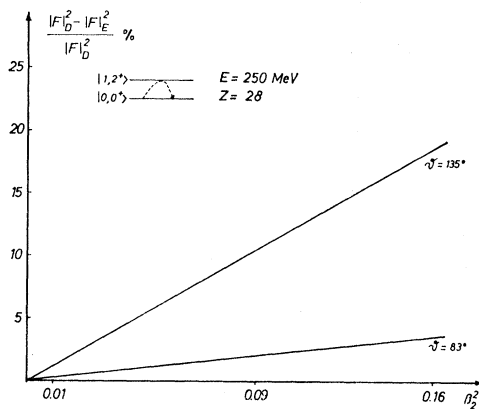


FIG. 4. Dependence of the dispersion effect

$$\left(\frac{|F|_{D^2} - |F|_{E^2}}{|F|_{D^2}} \right) / |F|_{D^2}$$

for elastic scattering on the square of the effective deformation β_2 at scattering angles near the minima of $|F|_{D^2}$.

³⁸ A similar calculation at $E=175$ MeV shows that this is indeed an effect depending on the scattering angle in this energy region.

³⁹ $H_{cc'}$ becomes zero in our model, as long as no reorientation (Sec. VII) is considered.

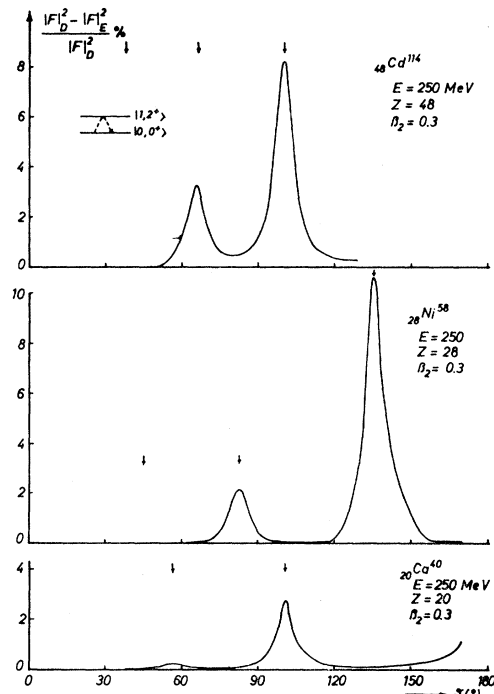


FIG. 5. Dispersion effect in elastic scattering for Ca^{40} , Ni^{58} , and Cd^{114} . The small arrows above the abscissa indicate the position of the minima of $|F|_{D^2}$.

We discussed already in Sec. III the dependence of the dispersion effect on the energy of the intermediate states, which was found to enter only through the matrix elements and is therefore weak. In this calculation, this dependence vanishes completely, since we neglected retardation and consequently the energy loss of the electron.

Another question is how much the dispersion effect depends on the $B(E\lambda)$ values of the virtual transitions. We considered again a 2^+ state as intermediate state and calculated the dispersion effect for various effective deformations β_2 . From (75), we expect ΔS^I to be proportional to β_2^2 . Since in elastic scattering \tilde{S}^I is independent of β_2 , we expect from (74) that the dispersion effect will be proportional to β_2^2 . This proportionality is confirmed by our actual calculations (Fig. 4).

Because $\beta_2^2 \sim B(E\lambda)$, one may make the generalization that for every intermediate state the dispersion effect is proportional to the $B(E\lambda)$ of the corresponding virtual transition, as long as the other parameters entering in the definition of $B(E\lambda)$ [Eq. (60)], i.e., Z and R_0 , are fixed. No quantitative theoretical predictions can be made on the dependence of the dispersion effect on these parameters, since the DWBA S matrices \tilde{S}^I themselves depend in an involved way on Z and R_0 . Qualitatively one expects, however, that the dispersion effect becomes smaller when the target nucleus becomes heavier, because the minima of the cross sections are

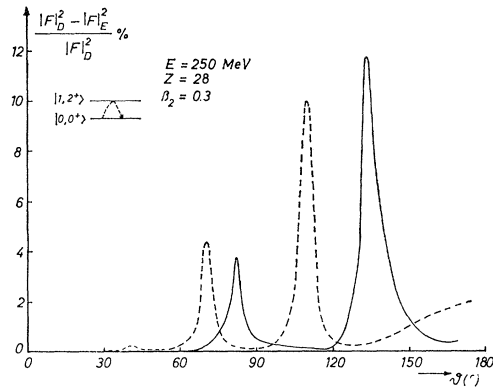


FIG. 6. Dispersion effect in elastic scattering for two nuclear models. Full line: Fermi-type charge distribution with $c=c_{tr}=4.28$ fm, $t=t_{tr}=2.49$ fm. Broken line: equivalent uniform charge distribution with $R_{eq}=5.071$ fm, $R_{tr}=4.45$ fm.

more pronounced in light target nuclei.⁸ This is confirmed by a calculation of the dispersion effects for $^{20}\text{Ca}^{40}$, $^{28}\text{Ni}^{58}$, and $^{48}\text{Cd}^{114}$ at $E=250$ MeV, where a 2^+ state with $\beta_2=0.3$ is taken into account as the intermediate state (Fig. 5). For a more extreme example, we also calculated the dispersion effect for the scattering of 200-MeV electrons by unpolarized $^{68}\text{Er}^{166}$, where the 2^+ state of the rotational band is taken as the intermediate state with $\beta_2=0.3$. In this case the dispersion effect never exceeds 1%.

To test the model dependence of the dispersion effect, we made two calculations for the scattering of 250-MeV electrons by Ni^{58} , taking both times a 2^+ vibrational state with $\beta_2=0.3$ as the intermediate state. First we calculated the dispersion effect, using (as before) a Fermi-type static charge distribution with $c=4.28$ fm and $t=2.49$ fm, and the corresponding transition charge potential (61); then we calculated the same quantity using the equivalent uniform static charge distribution with $R_{eq}=5.071$ fm and a δ -function transition density at $R_{tr}=5.545$ fm. Figure 6 shows that the value of the dispersion effect does not much depend on the nuclear model; the position of its maxima is, however, model-dependent: Since we defined the dispersion effect as a relative effect, its maxima occur at those scattering angles where the first-order form factors, which is of course model-dependent, has minima.

Up to this point we have considered primarily those properties of the dispersion effect which depend on the nature of the target. We will now turn to the influence of the kinematics of the scattering process on the dispersion effect.

B. Dependence on Momentum Transfer q and Incident Electron Energy E

Employing the same nuclear model as in Fig. 3, we calculated the dispersion effect for various energies of the electron and plotted it in Fig. 7 as a function of

both $100 \leq E \leq 250$ MeV and the momentum transfer q . The dispersion effect has its maxima where the form factors themselves have their minima. For fixed q the height of these maxima depends very little on E . A large electron energy is needed, however, to reach high momentum transfer q where the effect becomes large.

The parameters c and t of the Fermi-type charge distribution (50) were found for a number of spherical nuclei with $Z \geq 20$ by fitting to electron scattering experiments with energies up to about 250 MeV and scattering angles up to 120° ,² i.e., in regions of momentum transfer where the dispersion effects are still small enough to be neglected ($\leq 5\%$). Recent experiments at higher energies could not, however, be fitted by a first-order calculation with these parameters at backward angles with a momentum transfer $q \geq 1$ GeV/ c .⁴⁰ Since our results indicate that the dispersion effects become important for large momentum transfers, they should therefore be included, as well as the finer details of the electrostatic charge distribution, in the analysis of high-energy electron scattering data. This would not affect those conclusions, such as the nuclear radii and surface thicknesses, which are drawn from the forward part of the diffraction pattern, where the momentum transfer and thus the dispersion effects are small.

VI. DISPERSION EFFECT IN INELASTIC SCATTERING

Since we always calculate the entire S matrix we get the inelastic cross sections for the excitation of all

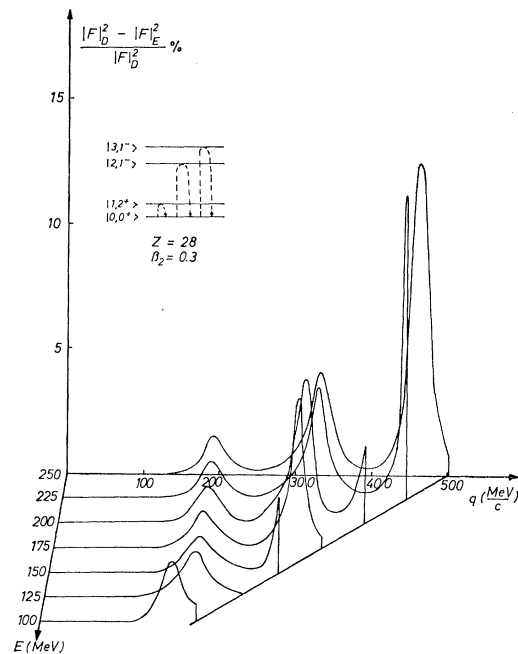


FIG. 7. Dispersion effect in elastic scattering as a function of the incident electron energy E and the momentum transfer q . The nuclear model is described in Fig. 3.

⁴⁰ J. B. Bellicard *et al.*, Phys. Rev. Letters 19, 527 (1967).

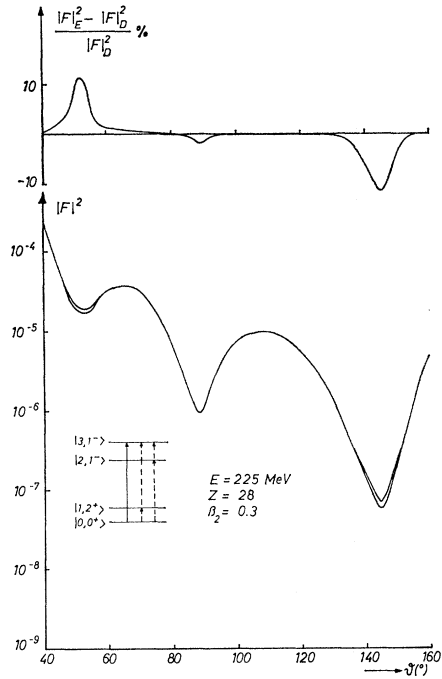


FIG. 8. Form factors and the dispersion effect for the excitation of the $|3, 1^- \rangle = (-\frac{1}{2}d^\dagger + \frac{1}{2}\sqrt{3}[d^\dagger \times \beta^\dagger]^{1-1}) |0 \rangle$ state in Ni^{68} . In the spectrum, the full arrow indicates the first-order transition, and the broken arrows show the major virtual transitions.

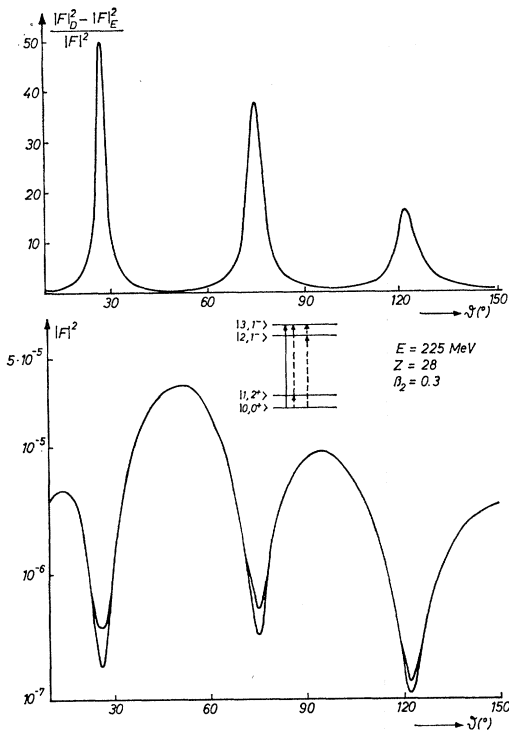


FIG. 9. Same as Fig. 8, except for the giant-resonance wave functions $|2, 1^- \rangle = d^\dagger |0 \rangle$, $|3, 1^- \rangle = [d^\dagger \times \beta^\dagger]^{1-1} |0 \rangle$.

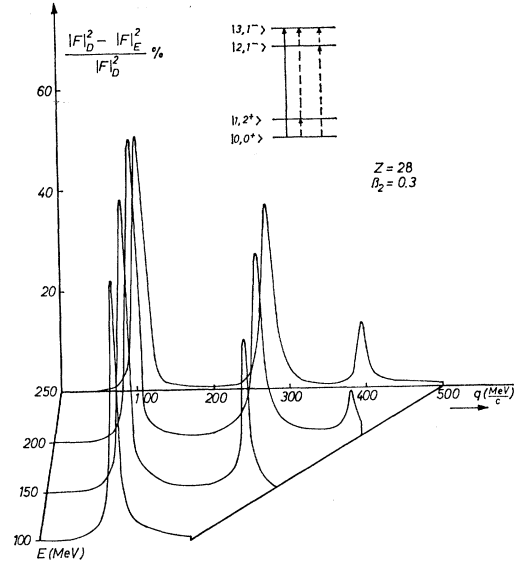


FIG. 10. Same as Fig. 9 for various incident electron energies E as a function of E and the momentum transfer q .

nuclear states, which were taken into account as intermediate states together with the elastic cross section. In Fig. 8 we show as an example the form factors and the dispersion effect for the excitation of the upper giant-resonance state (68):

$$|\alpha, J\rangle = |3, 1^- \rangle = (-\frac{1}{2}d^\dagger + \frac{1}{2}\sqrt{3}[d^\dagger \times \beta^\dagger]^{1-1}) |0 \rangle. \quad (76)$$

Since we defined the dispersion effect as a relative effect, $(|F|_{D^2} - |F|_{E^2}) / |F|_{D^2}$, we can increase it by making the first-order effect smaller. If, for example, we choose the admixture coefficients in the wave functions of the giant-resonance states in such a manner that the dipole and the quadrupole modes are decoupled:

$$|\alpha, J\rangle = |3, 1^- \rangle = [d^\dagger \times \beta^\dagger]^{1-1} |0 \rangle, \quad (77)$$

then the $|3, 1^- \rangle$ state can even in first order only be reached from the ground state by the excitation of both a dipole and a quadrupole phonon. The form factor $|F|_{D^2}$ therefore becomes smaller than in the (realistic) coupled case, and the dispersion effect becomes larger (Fig. 9). These calculations were repeated for several energies E (Fig. 10).

TABLE II. Same as in Table I for the excitation of the $|3, 1^- \rangle$ state.

Intermediate states (deg)	$ 1, 2^+ \rangle$ (%)	$ 2, 1^- \rangle$ (%)	$\begin{matrix} 1, 2^+ \rangle \\ 2, 1^- \rangle \end{matrix}$ (%)
$\theta = 52$	6.3	3.5	10.8
$\theta = 90$	-0.8	-1.1	-1.9
$\theta = 145$	-8.0	-5.3	-13.0

As in elastic scattering, we find by neglecting the $|1, 2^+\rangle$ intermediate state or the $|2, 1^-\rangle$ intermediate state that the matrix elements of ΔS^T are a sum of the contributions from the various possible intermediate states. These contributions then add up also for the total value of the dispersion effect (Table II), but in different ways at different angles because of the coherent partial-wave sum in (75).

Before investigating the dependence of the dispersion effect in inelastic scattering on the transition strengths of the virtual excitations, we will consider a type of higher-order effect other than the dispersion effect. The latter comes from a virtual excitation to an intermediate state $|\alpha, J^\pm\rangle$, which differs in its quantum number α from both the initial and final states. In contrast to the dispersion effect, the so-called reorientation effect comes from virtual transitions between the various magnetic substates of a particular nuclear state. It is well known and experimentally studied in Coulomb excitation.⁴¹ We can investigate the corresponding effect in electron scattering by assuming an anharmonic-vibrator model for the nucleus.

VII. REORIENTATION EFFECT

In the vibrator model of a spherical nucleus we consider the following excited states (Fig. 11) a singlet state,

$$|1, 2^+\rangle = (p_1\beta^\dagger + q_1/\sqrt{2}[\beta^\dagger \times \beta^\dagger]^{[2^+]})|0\rangle, \quad (78)$$

and the triplet

$$|2, 2^+\rangle = (p_2\beta^\dagger + q_2/\sqrt{2}[\beta^\dagger \times \beta^\dagger]^{[2^+]})|0\rangle, \quad (79)$$

$$|3, 0^+\rangle = 1/\sqrt{2}[\beta^\dagger \times \beta^\dagger]^{[0^+]})|0\rangle, \quad (80)$$

$$|4, 4^+\rangle = 1/\sqrt{2}[\beta^\dagger \times \beta^\dagger]^{[4^+]})|0\rangle. \quad (81)$$

The mixing of the one-phonon 2^+ and the two-phonon 2^+ states describes an anharmonicity in the nuclear quadrupole vibrations, which leads to static quadrupole moments in the 2^+ states:

$$eQ = \left(\frac{16\pi}{5}\right)^{1/2} \left\langle \alpha, 2^+ \left| \int d\tau \rho_N(\mathbf{r}) r^2 Y_{2,0} \right| \alpha, 2^+ \right\rangle. \quad (82)$$

Inserting (56), one gets, after some calculations,

$$Q = 16 \left(\frac{\pi}{35}\right)^{1/2} Z N_2 p_\alpha q_\alpha \int dr r^5 \frac{d\rho_0}{dr} + \frac{4}{7} Z N_2^2 (2p_\alpha^2 - \frac{8}{7}q_\alpha^2) \int dr r^6 \frac{d^2\rho_0}{dr^2}, \quad (83)$$

and the reduced transition probabilities become

$$\begin{aligned} B(E2, |0, 0^+\rangle \rightarrow |\alpha, 2^+\rangle) &= \left| \left\langle \alpha, 2^+ \left| \int d\tau r^2 \rho_N(\mathbf{r}) Y_2 \right| 0 \right\rangle \right|^2 \\ &= 5 \left[-Z e N_2 p_\alpha \int dr r^5 \frac{d\rho_0}{dr} \right. \\ &\quad \left. - Z e N_2^2 q_\alpha \left(\frac{5}{7\pi}\right)^{1/2} \int dr r^6 \frac{d^2\rho_0}{dr^2} \right]^2. \quad (84) \end{aligned}$$

We consider the excitation of the $|1, 2^+\rangle$ state. The direct-transition potential is obtained from (46), (56), and (78) and is given, up to two-phonon terms, by

$$\begin{aligned} J_{0,0^+ \rightarrow 1,2^+}^{(2)} &= Z e^2 (\sqrt{5}) \int_0^a dr r^2 \frac{r^{\leq 2}}{r^3} \\ &\times \left[-N_2 p_1 r \frac{d\rho_0}{dr} - N_2^2 q_1 \left(\frac{5}{7\pi}\right)^{1/2} r^2 \frac{d^2\rho_0}{dr^2} \right]. \quad (85) \end{aligned}$$

It is consistent to consider only one-phonon terms in the transition potentials of the virtual transitions because they enter at least quadratically into the S matrix. In order to get the form factor $|F|_{E^2}$ for the excitation of

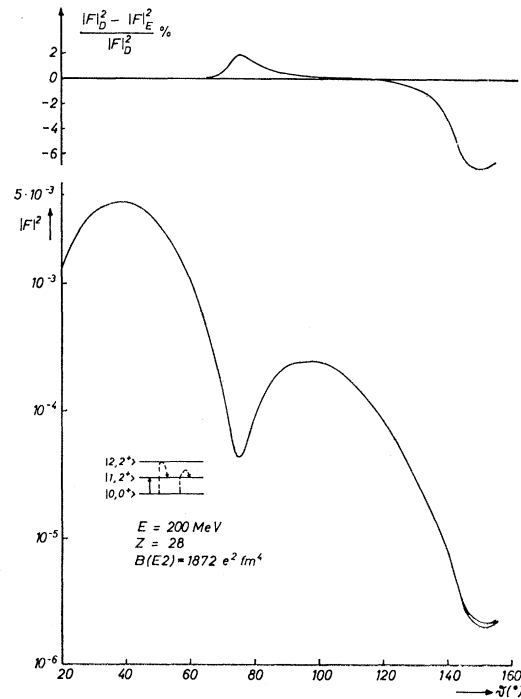


FIG. 11. Total higher-order effect in Ni^{58} for the excitation of the $|1, 2^+\rangle$ state with wave functions $|1, 2^+\rangle = (\frac{1}{2}\sqrt{3}\beta^\dagger + \frac{1}{2}[\beta^\dagger \times \beta^\dagger]^{[2^+]})|0\rangle$ and $|2, 2^+\rangle = (-\frac{1}{2}\beta^\dagger + \frac{1}{2}\sqrt{3}[\beta^\dagger \times \beta^\dagger]^{[2^+]})|0\rangle$. The unbroken line represents the first-order transition, the broken line ($|0, 0^+\rangle \rightarrow |2, 2^+\rangle \rightarrow |1, 2^+\rangle$) represents the dispersion effect, and the broken line ($|0, 0^+\rangle \rightarrow |1, 2^+\rangle \rightarrow |1, 2^+\rangle$) represents the reorientation effect.

⁴¹ J. de Boer and J. Eichler, in *Advances in Nuclear Physics* (Plenum Press, Inc., New York, 1968), Vol. 1. This review article contains more references.

the $|1, 2^+\rangle$ state exactly up to terms of order β_2^2 , we can then drop the 0^+ and the 4^+ state of the triplet and also all transition potentials with $\lambda \neq 2$, and we are left with

$$J_{0,0^+ \rightarrow 2,2^+}^{(2)} = Ze^2(\sqrt{5}) \int_0^a dr r^2 \frac{r <^2}{r >^3} - (p_2) N_{2r} \frac{d\rho_0}{dr}, \quad (86)$$

$$J_{1,2^+ \rightarrow 2,2^+}^{(2)} = Ze^2(\sqrt{10}) \int_0^a dr r^2 \frac{r <^2}{r >^3} \times (-p_1 q_2 - q_1 p_2) N_{2r} \frac{d\rho_0}{dr}, \quad (87)$$

$$J_{1,2^+ \rightarrow 1,2^+}^{(2)} = Ze^2 2(\sqrt{10}) \int_0^a dr r^2 \frac{r <^2}{r >^3} (-p_1 q_1) N_{2r} \frac{d\rho_0}{dr}. \quad (88)$$

The latter describes a transition within the magnetic substates of the $|1, 2^+\rangle$ state. Because transitions between states with different magnetic quantum numbers are possible, such a transition is called a reorientation. Figure 11 shows the result of our calculation for $Z=28$. The total higher-order effect is a sum of the dispersion effect, i.e., the two-step excitation $|0, 0^+\rangle \rightarrow |2, 2^+\rangle \rightarrow |1, 2^+\rangle$, and the reorientation effect $|0, 0^+\rangle \rightarrow |1, 2^+\rangle \rightarrow |1, 2^+\rangle$. Table III shows that the dispersion effect and the reorientation effect are of opposite sign. This was also found in the Coulomb excitation of Er^{166} ,⁴² where the 2^+ state of the rotation band takes the role of our $|1, 2^+\rangle$ state and the ground state of the γ band takes the role of our $|2, 2^+\rangle$ state.

For the dependence of the effect on the effective deformation β_2 , we note that if $\beta_2 \ll 1$, then \tilde{S}^T is proportional to β_2 [Eq. (27)] and ΔS^T to β_2^2 [Eq. (75)], because the one-phonon term gives the major contribution to $J_{0,0^+ \rightarrow 1,2^+}^{(2)}$. Therefore, both the dispersion effect and the reorientation effect are proportional to β_2 (Fig. 12).

Furthermore, we repeated the calculation, which led to Fig. 11, for ${}_{48}\text{Cd}^{114}$. Although $B(E2, |0, 0^+\rangle \rightarrow |1, 2^+\rangle)$

TABLE III. Total higher-order effect in the excitation of the $|1, 2^+\rangle$ state in Ni^{58} at $E=200$ MeV near the minima of $|F|_{D^2}$. The second column gives the dispersion effect, and the third gives the reorientation effect. In the fourth column, both virtual excitation modes were considered to give the total effect. The wave functions are $|1, 2^+\rangle = (\frac{1}{2}\sqrt{3}\beta_1^\dagger + \frac{1}{2}[\beta_1^\dagger \times \beta_1^\dagger]^{(2^+)}) |0\rangle$ and $|2, 2^+\rangle = (-\frac{1}{2}\beta_1^\dagger + \frac{1}{2}\sqrt{3}[\beta_1^\dagger \times \beta_1^\dagger]^{(2^+)}) |0\rangle$.

Intermediate states (deg)	$ 2, 2^+\rangle$ (%)	$ 1, 2^+\rangle$ (%)	$\begin{matrix} 2, 2^+\rangle \\ 1, 2^+\rangle \end{matrix}$ (%)
$\theta=75$	-1.4	3.4	1.9
$\theta=150$	+2.7	-10.0	-7.4

⁴² B. Greiner and H. Arenhövel, Nucl. Phys. **A107**, 225 (1968); A. C. Douglas and N. MacDonald, Phys. Letters **24B**, 447 (1967).

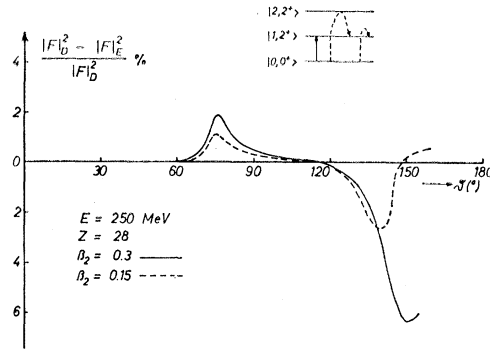


FIG. 12. Same as in Fig. 11 for various β_2 .

is larger than in the previous case, we find the total higher-order effect much smaller (Fig. 13). The reason for this is again that for large Z the form factor $|F|^2$ becomes a smoother function of the scattering angle θ .

VIII. NUMERICAL TESTS OF PROGRAM AND COMPARISON WITH OTHER CALCULATIONS

The numerical exactness of the underlying DWBA program is obviously essential for our EKT calculation. This program has been used and tested in various calculations.²¹⁻²³ We can reproduce the elastic Born-approximation form factor for $E=250$ MeV up to $\theta=150^\circ$ (which is farther backwards than the last minimum at $\theta=135^\circ$ in Fig. 3) with an error smaller than 10% by setting $Z=0.1$ when calculating the wave function of the electron. It is important to find a good value for the radius R_{as} , at which the numerically integrated wave functions are fitted to the point Coulomb wave functions for the evaluation of the potential scattering phase. Because of the tail of the electrostatic Fermi-type charge distribution, this radius must not be chosen too small; on the other hand, it is difficult to calculate the point Coulomb functions accurately if R_{as} is too large. We found that at $E=250$ MeV, $R_{as}=8.25$ fm gives optimal results for Ni^{58} . When we intentionally changed this value to $R_{as}=10.25$ fm, we found that the form factor $|F|_{D^2}$ itself was changed by 21% at $\theta=135^\circ$ (Fig. 3), while the dispersion effect $(|F|_{D^2} - |F|_{E^2}) / |F|_{D^2}$ was changed from the value 11.4% of Fig. 3 to 17%. It seems, therefore, that the dispersion effect, though it is a difference effect, can be calculated fairly accurately with our program even at backward-scattering angles.

To have an independent check on the validity of the EKT approach, we compared our calculations with Rawitscher's coupled-channel results.⁷ A virtual monopole excitation is considered, with a transition charge density

$$\rho_{tr} = \langle 0, 0^+ | \rho_N | 1, 0^+ \rangle = N(B + x^2 e^{-x}), \quad (89)$$

where

$$x = r/z \quad (90)$$

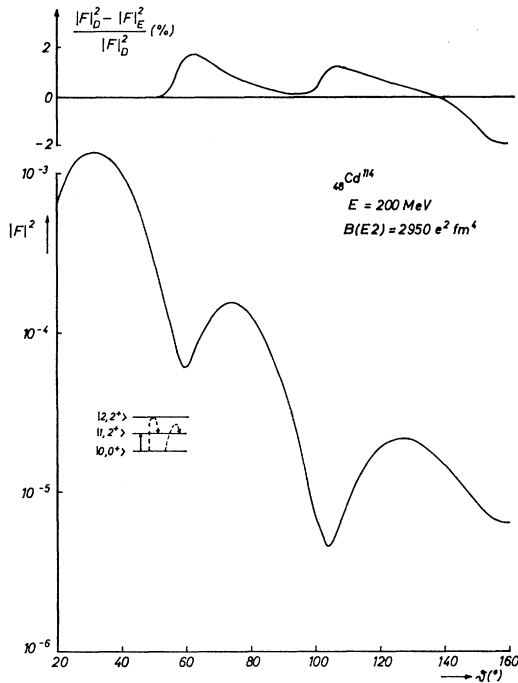


FIG. 13. Same as in Fig. 11 for Cd^{114} , where with our wave functions the quadrupole moment in the $|1, 2^+\rangle$ state becomes $Q = -55.3 \text{ fm}^2$.

(z being a parameter) and B is determined in terms of a cutoff radius R from the condition

$$\int_0^R \rho_{\text{tr}}(r) r^2 dr = 0. \quad (91)$$

The normalization constant is adjusted in such a manner that the total inelastic cross section has a certain value. Figure 14 shows Rawitscher's coupled-channel results and the EKT results for the scattering of 250-MeV electrons by Ca^{40} . As usual, we have the maxima of the absolute value of the dispersion effect there and only there, where the elastic form factor itself has minima. At these extrema there is an excellent agreement between both calculations. We cannot, however, reproduce the two smaller extrema which occur in the coupled channel result.

No direct comparison is possible between our results and those of the second-order DWBA calculation of Onley,⁸ because closure is used for the intermediate states in the latter. But as far as the sign and the order of magnitude are concerned, there is good qualitative agreement between Fig. 3 and Onley's corresponding result.

IX. CONCLUSIONS

We have shown that it is quite simple to calculate higher-order effects in electron scattering by using the eigenchannel theory, because any DWBA program has only to be extended by a diagonalization procedure to give the higher-order cross sections. Since the coupling between the various channels is small, one can calculate

the matrix S , which includes the higher-order effects, with one iteration out of the first-order matrix S . One needs, therefore, only slightly more time to compute the cross sections for electron-nucleus scattering including higher-order effects due to virtual transitions between the various channels than to compute the cross section for the scattering into these channels in first-order perturbation theory.

In elastic scattering we get effects of the order of 12% at $E = 250 \text{ MeV}$ and backward angles. This value is, of course, too small to be detected experimentally. It seems, however, that the dispersion effect is at least partially responsible for the disagreement between the low-energy fits of the parameters of the electrostatic nuclear charge distributions and recent high-energy experiments.⁴⁰ Figure 7 suggests strongly that the dispersion effect becomes larger with larger momentum transfer q . It is therefore desirable to extend the calculations to higher energies. Such work is in progress.

Also, our results for inelastic scattering indicate that it will be difficult to measure higher-order effects, since these effects show up in the minima of the inelastic cross sections, while the most accurate experimental work is done for low-momentum transfer q in the ascending part of the inelastic form factor.^{43,44} The best chance to detect higher-order effects in inelastic scattering is, of course, given when the first-order transition is strongly hindered, as in Fig. 9, or even forbidden as for the excitation of a 0^- state from 0^+ ground state. In the latter case one of the virtual transitions has to be of magnetic type. Therefore the transverse parts of the electromagnetic interaction have to be included in such a calculation. Moreover, the retardation and the energy loss of the electron should be taken into account to get exact results at backward angles. Existing DWBA programs⁴⁵ in which these effects are taken care of can be used as a basis for an EKT calculation.

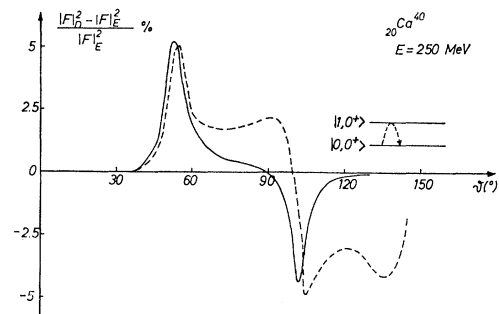


FIG. 14. Comparison of Rawitscher's coupled-channel result (broken line) with the corresponding EKT result (unbroken line) for the dispersion effect in the elastic scattering of 250-MeV electrons by Ca^{40} with a virtual monopole excitation.

⁴³ F. Gudden and P. Strehl, *Z. Physik* **185**, 111 (1965); M. Stroetzel, *ibid.* **214**, 357 (1968).

⁴⁴ M. A. Duguay, C. K. Bockelman, T. H. Curtis, and R. A. Eisenstein, *Phys. Rev.* **163**, 1259 (1967); J. F. Ziegler and G. A. Peterson, *ibid.* **165**, 1337 (1968); G. A. Peterson and J. Alster, *ibid.* **166**, 1136 (1968).

⁴⁵ J. F. Ziegler, Yale Report No. 2726 E-49, 1967 (unpublished); S. T. Tuan, H. J. Weber, and L. E. Wright, *Phys. Rev.* **167**, 939 (1968); D. Drechsel, *Nucl. Phys.* **113**, 665 (1968).

Besides the retardation, the only other approximation in this work is the neglect of the interior basis state with a radial quantum number $n \neq 0$. We showed, however, in Sec. II that these neglected states couple about 20 times more weakly to the first-order transition than the weakest-coupling channels that were taken into account.

Another open question is, of course, whether our nuclear model, which is, of course, very schematic, gives an appropriate representation of the possible virtual states. We take only a few discrete states of the whole spectrum of electron-nucleus scattering into account, namely, those such that the energy loss of the electron is $E \leq 20$ MeV. This is justified as long as one is interested in order-of-magnitude results and deals with moderate incident electron energies. If, however, the incident energy of the electron becomes large, then virtual excitations into the quasi-elastic peak, or even virtual meson production, could play a role in the dispersion effect, inasmuch as we found that the dispersion effect depends on the energy loss of the electron in a virtual excitation only through the interaction matrix elements (Sec. III). Moreover, these states form a continuum (as does the giant resonance in a more realistic model). The nuclear continuum problems which arise in electron scattering have recently been treated by applying the EKT to a nuclear shell-model Hamiltonian, while the electron was treated in Born

approximation.⁴⁶ To include higher-order effects one has to apply the EKT to both the electron and the escape nucleon. Such a two-particle EKT has also been formulated.⁴⁷

An actual calculation of this type will, however, be very involved. It therefore seems advantageous to consider the closed forms (42) (in which no explicit reference is made to the intermediate states) or (41) (which can be evaluated by the use of sum rules) for further applications of the eigenchannel theory to electron scattering.

ACKNOWLEDGMENTS

Our calculations are based on DWBA program which was lent us by Dr. D. Drechsel. We thank him and Dr. W. Scheid for many discussions and for helpful advice. The numerical work was done with the Burroughs 5500 at the Computer Science Center of the University of Virginia. We acknowledge the kind cooperation of its staff. Furthermore, we gratefully acknowledge the kind hospitality of Professor W. D. Whitehead at the Center for Advanced Studies of the University of Virginia.

⁴⁶ P. Antony-Spies, W. Donner, H. G. Wahsweiler, and W. Greiner, Phys. Letters **26B**, 268 (1968).

⁴⁷ M. Danos and W. Greiner, Z. Physik **202**, 125 (1967); H. J. Weber and W. Greiner, University of Virginia Report, 1968 (unpublished).

Measurement of Polarization Effects in the $H^2(d, p)H^3$ Reaction at 140 keV*†

R. I. STEINBERG, C. W. DRAKE,‡ AND D. C. BONAR
Gibbs Laboratory, Yale University, New Haven, Connecticut 06520
(Received 26 May 1969)

The vector analyzing power $D_2(\theta)$ and the tensor analyzing powers $D_{22}(\theta)$ and $[D_{11}(\theta) - D_{22}(\theta)]$ of the $H^2(d, p)H^3$ reaction have been measured at a mean deuteron energy of 140 keV using a beam of polarized deuterons from the Yale polarized-ion source and a 100-keV-thick target of unpolarized deuterated polyethylene. The results for the vector analyzing power are in agreement with previous measurements by Ad'yasevich *et al.* at 100 and 200 keV and are consistent with a theoretical treatment by Rook and Goldfarb. In the notation of this treatment, the results are $B_2/B_0 = 0.321 \pm 0.059$ and $B_4/B_0 = -0.036 \pm 0.042$. The results for the tensor analyzing powers are in reasonable agreement with a previous measurement by Ad'yasevich *et al.* at 165 keV and are not consistent with the Rook-Goldfarb treatment in that a small contribution from quintet-state reaction matrix elements is apparent. The experimental results for the tensor analyzing powers are given by $B_6/B_0 = -0.059 \pm 0.015$, $B_6'/B_0 = -0.556 \pm 0.102$, and $B_7/B_0 = -0.413 \pm 0.152$. The quintet-state contributions, in the notation introduced in this paper, are measured to be $B_8/B_0 = -0.148 \pm 0.084$ and $B_{11}/B_0 = 0.002 \pm 0.009$. A calculation is made in which the assumptions of the Rook-Goldfarb treatment are relaxed in order to allow nonvanishing s -wave quintet-state reaction matrix elements. Explicit expressions for the various contributions of these reaction matrix elements to the differential cross section are presented.

I. INTRODUCTION

SINCE its discovery by Lawrence, Livingston, and Lewis¹ in 1933, the $H^2(d, p)H^3$ reaction has been

* Research supported by the U.S. Atomic Energy Commission.

† Based on a dissertation submitted by R.I.S. to the faculty of Yale University in candidacy for the Ph.D. degree.

‡ Present address: Oregon State University, Corvallis, Ore. 97331.

¹ E. O. Lawrence, M. S. Livingston, and G. N. Lewis, Phys. Rev. **44**, 56(L) (1933).

the subject of a great number of investigations, both theoretical and experimental. The main point of interest for the earliest work was the 1936 discovery² that the angular distribution of the outgoing protons was anisotropic in the c.m. system even at energies as low as 100 keV. This fact indicated that p -wave contributions to the reaction were important at these low energies.

² A. E. Kempton, B. C. Browne, and R. Maasdorp, Proc. Roy. Soc. (London) **A157**, 386 (1936).